

Axial and Equatorial Hydrogen Bonds: Jet-Cooled Rotational Spectrum of the Pentamethylene Sulfide \cdots Hydrogen Fluoride Complex

Susana Blanco, Alberto Lesarri, Juan C. López, and José L. Alonso*^[a]

Abstract: Two different axial and equatorial hydrogen-bonded conformers of the complex formed by pentamethylene sulfide and hydrogen fluoride have been generated in a pulsed supersonic expansion and characterised by means of Fourier transform microwave spectroscopy. The ground-state rotational spectra of six isotopomers ($C_5H_{10}S \cdots HF$, $C_5H_{10}S \cdots DF$, $C_5H_{10}^{34}S \cdots HF$, $^{13}C_\alpha C_4H_{10}S \cdots HF$, $^{13}C_\beta C_4H_{10}S \cdots HF$ and $^{13}C_\gamma C_4H_{10}S \cdots HF$) have been analysed for both conformers in the frequency range 5.5–18.5 GHz. The rotational parameters were used to derive C_s struc-

tures for the conformers, with hydrogen fluoride pointing to the domain of the nonbonding electron pairs at either the axial or equatorial position of the sulfur atom. The axial form was found to be the more stable, in contrast with the observation for the pentamethylene sulfide $\cdots HCl$ complex. No equatorial-to-axial relaxation was observed when He or Ar were used as the carrier gas. The

Keywords: conformation analysis • hydrogen bonds • rotational spectroscopy • supersonic jet

conformational behaviour is compared with that of related six-membered rings and discussed in terms of the existence of secondary hydrogen bonding between the halogen atom and the nearest H atoms of the methylene groups of the ring. No significant structural distortion of pentamethylene sulfide upon complexation was detected from a comparison with the structure of the isolated monomer. Finally, an ab initio study was carried out to complement the experimental results.

Introduction

Molecular conformation plays a crucial role in chemistry and biochemistry. Hydrogen-bond interactions, both intra- and intermolecular, are ubiquitous and critical in determining the conformation of molecular complexes. Hydrogen-bonded complexes in the gas phase are usually produced in pulsed supersonic beams where the intrinsic properties of complexes are obtained in the collisionless expansion. Contemporary research into hydrogen bonding aims to obtain accurate structural parameters through a combination of spectroscopic techniques and supersonic beams.^[1] A very powerful technique to determine the conformation and structure of small clusters is molecular beam Fourier transform microwave spectroscopy (MB-FTMW).^[2] It allows the characterisation of specific molecular complexes even if they consist of mixtures of different conformers, since their individual rotational spectra can be characterised in the collisionless region of the jet. Furthermore, in all cases the structural parameters

characterising the hydrogen bond can be determined very precisely from the experimental spectroscopic constants.

In spite of the large number of hydrogen-bonded molecular complexes studied up to the present, the first observation of different hydrogen-bonded axial and equatorial conformers has only recently been reported by us; they occur in the tetrahydropyran (THP) and pentamethylene sulfide (PMS) complexes with HCl and HF.^[3–5] Both six-membered rings can be considered as prototype systems since they present two nonbonding electron pairs at the O or S atoms that turn out to be nonequivalent due to the chair conformation of the rings. The hydrogen atom in HX (where X = F, Cl) is electrophilic and seeks the most nucleophilic site of O or S, which will be along the direction of the nonbonding electron pairs. Consequently, the formation of hydrogen bonds gives rise to two different axial and equatorial conformers, as depicted in Figure 1.

In the cases of THP $\cdots HCl$ ^[3] and THP $\cdots HF$,^[5] the axial form was found to be the most stable. In contrast, a preference for the equatorial form was observed in PMS $\cdots HCl$.^[4] It has been shown that this axial/equatorial conformational preference may be controlled by secondary interactions between the halogen Cl/F atom and the nearest H atoms of the methylene groups of the ring. Noticeable nonlinearity of the hydrogen bond in some cases provides evidence for this interaction. In the case of the bicyclic ether 6-oxabicyclo[3.1.0]hexane $\cdots HCl$ complex,^[6] the very short distance from the Cl atom to the

[a] Prof. Dr. J. L. Alonso, Prof. Dr. S. Blanco, Prof. Dr. A. Lesarri, Prof. Dr. J. C. López
Departamento de Química – Física
Facultad de Ciencias, Universidad de Valladolid
47071 Valladolid (Spain)
Fax: +34 983 423264
E-mail: jlonso@qf.uva.es

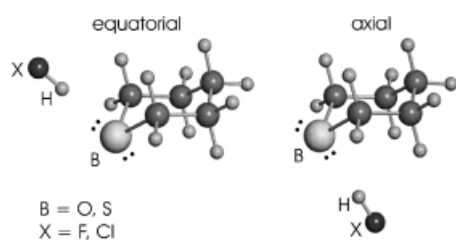


Figure 1. Axial and equatorial hydrogen-bond conformers PMS...HX and THP...HX.

closest H atoms in the ring makes the axial form unstable, and only the equatorial conformer was observed. Thus, a priori predictions of the most stable conformer seem to be difficult. A relaxation from the equatorial (high-energy) conformer to the axial (more stable) conformer observed in the THP complexes^[3, 5] can be attributed to a low barrier to the interconversion between them. However, a high barrier inhibits the conformational relaxation in the PMS...HCl complex.^[4] In the study of THP...HF,^[5] the structure of the THP monomer in the complex was determined, and it was possible for the first time to check the usual assumption of unchanged geometry of the monomers upon complexation.

Abstract in Spanish: Los conformeros axial y ecuatorial del complejo formado por enlace de hidrógeno entre las moléculas de sulfuro de pentametileno y fluoruro de hidrógeno se han observado en la expansión supersónica de mezclas gaseosas de estos componentes diluidos en un gas inerte (He o Ar). La caracterización de los dos conformeros se ha llevado a cabo empleando la técnica de espectroscopía de microondas con transformación de Fourier, que ha permitido observar su espectro de rotación en el intervalo de frecuencias 5–18,5 GHz. Se presentan los resultados del análisis del espectro de rotación de seis isotopómeros ($_5\text{H}_{10}\text{S}\cdots\text{HF}$, $\text{C}_5\text{H}_{10}\text{S}\cdots\text{DF}$, $\text{C}_5\text{H}_{10}^{34}\text{S}\cdots\text{HF}$, $^{13}\text{C}_\alpha\text{C}_4\text{H}_{10}\text{S}\cdots\text{HF}$, $^{13}\text{C}_\beta\text{C}_4\text{H}_{10}\text{S}\cdots\text{HF}$ and $^{13}\text{C}_\gamma\text{C}_4\text{H}_{10}\text{S}\cdots\text{HF}$), observados en abundancia natural, en el estado fundamental de vibración. Los parámetros de rotación son consistentes con estructuras de equilibrio C_s para ambos conformeros. Las estructuras calculadas indican que el HF forma enlaces de hidrógeno con el átomo de azufre en las regiones de los pares electrónicos no enlazantes del mismo, en posición axial o ecuatorial. Se ha encontrado que la especie axial es la más estable, en contraste con lo observado en el complejo sulfuro de pentametileno...HCl. Por otra parte, no se ha observado relajación de la forma ecuatorial a la axial independientemente del empleo de He o Ar como gas portador. La estabilidad relativa de los conformeros axial y ecuatorial se compara con la de otros complejos similares de HF o HCl con anillos de seis miembros, poniendo de manifiesto la relevancia de la existencia de enlaces de hidrógeno secundarios entre el halógeno y los átomos de hidrógeno más próximos de los grupos metileno del anillo. La comparación de las estructuras del sulfuro de pentametileno en el complejo y aislado ha permitido concluir que no existen distorsiones significativas de la estructura del monómero en la complejación. Por último, los resultados experimentales se han complementado con un estudio *ab initio* del complejo.

Very recently, we have also reported axial and equatorial hydrogen-bond complexes for trimethylene sulfide (TMS)...HCl.^[7] The four-membered ring of TMS (thietane) executes a ring-puckering large-amplitude motion, by which the two C_s puckered equilibrium conformations interconvert via tunnelling, making the nonbonding electron pairs at the sulfur atom equivalent. This equivalence is broken by the effect of complexation with HCl, giving rise to axial and equatorial conformers. In the complexes formed by the related oxetane (trimethylene oxide) with HCl^[8] and HF,^[9] only one conformer has been observed, since the planar configuration of the ring remains after complexation. In the case of hydrogen-bonded complexes of five-membered rings of tetrahydrofuran and tetrahydrothiophene with HCl^[10, 11] and HF,^[12, 13] two equivalent equilibrium conformations with pyramidal configurations at O or S have been found.

In the present work we report a detailed analysis of the hydrogen bond in the pentamethylene sulfide (PMS)...HF complex. As illustrated in Figure 1, two main binding sites can be anticipated, namely, at the axial and equatorial positions. The two conformers can be formed in a supersonic expansion and their geometries can be obtained. Possible changes in the axial/equatorial intensity ratio in spectra recorded with different carrier gases can be used to detect the existence of conformational relaxation between the conformers. The research on the PMS...HF complex was also directed at ascertaining the influence that secondary interactions have on the axial/equatorial conformational preference. The high sensitivity of our MB-FTMW spectrometer^[14] makes it possible to analyse the spectra of ^{34}S and ^{13}C isotopic species in their natural abundance, thus allowing the determination of the structure of the PMS monomer in the complex. By comparison of this structure with that of the isolated monomer, any noticeable structural distortion of PMS can be detected. The results of the present study are finally discussed in the context of those of related six-membered rings of THP and PMS complexes.

Results

Rotational spectra:

PMS monomer: The rotational spectrum of PMS has been previously studied,^[15, 16] but no structural data had been reported. In order to obtain a precise structure of the isolated monomer, we first undertook a rotational study of several isotopic species in their natural abundances. Owing to its C_s symmetry, PMS presents two sets of equivalent carbon atoms (α and β positions) and three different ^{13}C spectra with natural abundances of about 2% for $^{13}\text{C}_\alpha$ and $^{13}\text{C}_\beta$ species and 1% for $^{13}\text{C}_\gamma$ species (Figure 2). On the basis of the assignment of the parent species, R-branch transitions for all ^{13}C isotopic species were found near the predictions. In addition, the rotational spectrum of the ^{34}S isotopic species (natural abundance of about 4%) was also observed. The measured transitions for all isotopomers are collected in Table 1. The spectroscopic constants shown in Table 2 were derived by fitting the observed transitions for each isotopomer to Watson's asymmetric reduced Hamiltonian in the III' representation.^[17]

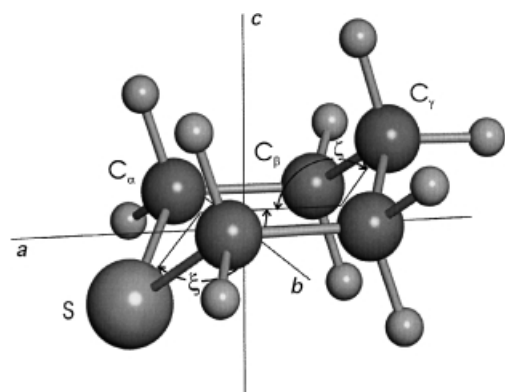


Figure 2. Structure of pentamethylene sulfide.

The fifteen rotational constants of Table 2 were used to determine the PMS structure. The substitution structure r_s of Column 1 in Table 3 was calculated by means of Kraitchman's equations,^[18] and the effective structure r_o of Column 2 was determined by a least-squares fitting procedure.^[19]

Axial PMS...HF: Guided by structural predictions made using the PMS structure of Table 3 and the reported structure of HF,^[20] we estimated trial rotational constants for the axial conformer. The geometrical parameters of the hydrogen bond were taken from the tetrahydrothiophene...HF complex.^[13] A near-prolate asymmetric rotor was predicted with dominant *a*-type R-branch transitions, along with a much less intense *b*-type spectrum. The region 11.9–12.3 GHz was initially

Table 1. Rotational transitions [MHz] for pentamethylene sulfide.

J'	K'_{-1}	K'_{+1}	J''	K''_{-1}	K''_{+1}	$C_5H_{10}S$		$C_5H_{10}^{34}S$		$^{13}C_\alpha C_4H_{10}S$	
						obs	obs – calcd ^[a]	obs	obs – calcd	obs	obs – calcd
1	1	0	0	0	0	6998.579	–0.001			6933.263	0.001
2	0	2	1	0	1	9305.252	0.001	9158.385	–0.001	9243.262	0.000
2	1	2	1	1	1	8749.957	–0.000	8594.438	–0.001	8703.148	–0.001
2	1	1	1	1	0	10932.227	–0.000	10692.794	0.002	10905.092	–0.001
2	2	0	1	1	0	14428.737	–0.000	14344.606	–0.001	14256.613	0.000
2	2	1	1	1	1	14984.035	–0.001				
2	1	1	1	0	1	13010.256	–0.000				
3	0	3	2	0	2	13142.005	–0.001	12963.185	–0.003	13036.903	0.001
3	1	3	2	1	2	12842.626	0.003	12634.387	0.000	12760.368	0.002
3	1	2	2	1	1	15926.280	–0.001	15622.626	0.003	15855.083	–0.003
3	2	2	2	2	1	14761.628	–0.001	14465.414	0.004	14706.169	0.000
3	2	1	2	2	0	16381.233	0.000	15967.615	–0.004	16375.424	0.001
4	0	4	3	0	3	16879.350	0.000	16642.905	–0.001	16662.409	0.001
4	1	4	3	1	3	16780.344	–0.001	16524.334	0.001	16748.866	–0.001

J'	K'_{-1}	K'_{+1}	J''	K''_{-1}	K''_{+1}	$^{13}C_\beta C_4H_{10}S$		$^{13}C_\gamma C_4H_{10}S$	
						obs	obs – calcd	obs	obs – calcd
1	1	0	0	0	0			6942.285	–0.001
2	0	2	1	0	1	9216.535	–0.000	9189.224	0.000
2	1	2	1	1	1	8670.706	–0.001	8626.565	0.000
2	1	1	1	1	0	10849.611	0.000	10742.501	0.001
2	2	0	1	1	0	14263.827	0.000	14363.937	0.000
3	0	3	2	0	2	13007.966	–0.002	13000.627	0.002
3	1	3	2	1	2	12720.129	0.003	12677.570	0.000
3	1	2	2	1	1	15792.007	0.002	15686.370	0.001
3	2	2	2	2	1	14640.229	0.000	14526.779	0.002
3	2	1	2	2	0	16272.472	–0.001	16052.935	–0.005
4	0	4	3	0	3	16708.216	–0.001	16691.969	0.000
4	1	4	3	1	3	16615.294	0.000	16577.447	0.000

[a] Obs – calcd: Observed – calculated values from the rotational parameters in Table 2.

Table 2. Rotational parameters for pentamethylene sulfide.

	$C_5H_{10}S$	$C_5H_{10}^{34}S$	$^{13}C_\alpha C_4H_{10}S$	$^{13}C_\beta C_4H_{10}S$	$^{13}C_\gamma C_4H_{10}S$
$A^{[a]}$ [MHz]	3992.7361(12) ^[b]	3991.0264(18)	3931.7428(17)	3941.6360(18)	3992.1659(17)
B [MHz]	3005.84661(74)	2935.49841(78)	3001.52248(78)	2984.77231(79)	2950.12339(78)
C [MHz]	1914.7053(11)	1886.3147(11)	1900.5433(11)	1895.3125(12)	1892.1484(12)
Δ_J [kHz]	0.831(38)	0.823(38)	0.817(38)	0.805(38)	0.829(38)
Δ_{JK} [kHz]	[–1.8] ^[c]	[–1.8]	[–1.8]	[–1.8]	[–1.8]
Δ_K [kHz]	[1.1]	[1.1]	[1.1]	[1.1]	[1.1]
δ_J [kHz]	[–0.11]	[–0.11]	[–0.11]	[–0.11]	[–0.11]
δ_K [kHz]	[0.8]	[0.8]	[0.8]	[0.8]	[0.8]
$P_b^{[d]}$ [$u\text{\AA}^2$]	111.19420(35)	111.19299(36)	113.03825(36)	112.77142(36)	111.18865(36)
$\sigma^{[e]}$ [MHz]	0.001	0.002	0.001	0.001	0.002

[a] The coefficients A , B and C are the rotational constants; Δ_J , Δ_{JK} , Δ_K , δ_J and δ_K are the quartic centrifugal distortion constants. [b] Standard errors in parentheses in units of the last digit. [c] The centrifugal distortion constants Δ_{JK} , Δ_K , δ_J and δ_K were kept fixed to the values reported in ref. [16]. [d] $P_b = (I_a - I_b + I_c)/2 = \sum m_i b_i^2$. Conversion factor: $I_b \times B = 505\,379.1\text{ MHz } u\text{\AA}^2$. [e] Root mean square (rms) deviation of the fit.

Table 3. Structural parameters of pentamethylene sulfide.

Parameters ^[a,b]	r_s ^[c]	r_0
$r(\text{S}-\text{C}_\alpha)$ [Å]	1.8164(1) ^[d]	1.812(6)
$r(\text{C}_\alpha-\text{C}_\beta)$ [Å]	1.5156(1)	1.533(8)
$r(\text{C}_\beta-\text{C}_\gamma)$ [Å]	1.5311(1)	1.534(6)
$\angle \text{C}_\alpha\text{SC}_\alpha$ [°]	97.299(8)	97.8(4)
$\angle \text{SC}_\alpha\text{C}_\beta$ [°]	112.733(9)	112.5(5)
$\angle \text{C}_\alpha\text{C}_\beta\text{C}_\gamma$ [°]	112.407(9)	112.2(6)
$\angle \text{C}_\beta\text{C}_\gamma\text{C}_\beta$ [°]	112.956(9)	113.(6)
ξ [°]	130.64(2)	130.4(6)
ζ [°]	127.19(2)	127.(1)

[a] See Figure 2 for notation. [b] The remaining parameters were kept fixed at standard values of $r(\text{C}-\text{H}) = 1.095$ Å and $\angle \text{HCH} = 108.5^\circ$ (with a C_{2v} local symmetry around the C atoms). [c] The r_s coordinates for the S atom are $a = 1.42450(1)$ Å, $b = 0.0$ Å, $c = -0.17071(9)$ Å; for the C_α are $a = 0.34338(8)$ Å, $b = \pm 1.36349(2)$ Å, $c = 0.35030(9)$ Å; for the C_β are $a = -1.04269(3)$ Å, $b = \pm 1.27641(2)$ Å, $c = 0.2564(1)$ Å; for the C_γ are $a = -1.78099(2)$ Å, $b = 0.0$ Å, $c = 0.1560(2)$ Å. [d] Standard errors in parentheses in units of the last digit.

scanned using He as the carrier gas. This region was expected to contain the a -type R-branch $J = 4 \leftarrow 3$ transitions of the axial conformer with $K_{-1} = 0, 1, 2$ and 3. These were the first lines assigned. Subsequent scanning in the spectral region accessible with the spectrometer allowed the observation of the remainder a -type R-branch transitions. The spectra of the $\text{C}_5\text{H}_{10}\text{S} \cdots \text{DF}$, $\text{C}_5\text{H}_{10}^{34}\text{S} \cdots \text{HF}$, $^{13}\text{C}_\alpha\text{C}_4\text{H}_{10}\text{S} \cdots \text{HF}$, $^{13}\text{C}_\beta\text{C}_4\text{H}_{10}\text{S} \cdots \text{HF}$ and $^{13}\text{C}_\gamma\text{C}_4\text{H}_{10}\text{S} \cdots \text{HF}$ isotopomers were predicted from an assumed structure that reproduced the rotational constants of the parent species, and were analysed with the same procedure applied to the parent species.

Some of the observed transitions in the parent and isotopic species exhibited a hyperfine structure attributed to the interaction between the H and F nuclear spins within the HF subunit, with unresolved splittings less than 10 kHz apart. In addition, the isotopomer PMS \cdots DF presents a complicated hyperfine structure originating in the contribution of the D–F nuclear spin interaction within the DF subunit and the nuclear quadrupole coupling associated with a deuterium nucleus of spin $I = 1$. The splittings were not well resolved and central frequencies were considered in the fittings. Thus, the spectroscopic constants given in Table 4 were derived by fitting the observed transitions listed in Table 5 to Watson's asymmetric reduced Hamiltonian in the I' representation [Eq. (1)],^[17] where the coefficients A, B, C are the rotational constants

$$H_R^{(A)} = A \mathbf{P}_a^2 + B \mathbf{P}_b^2 + C \mathbf{P}_c^2 - \Delta_J \mathbf{P}^4 - \Delta_{JK} \mathbf{P}^2 \mathbf{P}_c^2 - \Delta_K \mathbf{P}_a^2 - 2\delta_J (\mathbf{P}^2 \mathbf{P}_b^2 - \mathbf{P}_c^2) - \delta_K [\mathbf{P}_a^2 (\mathbf{P}_b^2 - \mathbf{P}_c^2) + (\mathbf{P}_b^2 - \mathbf{P}_c^2) \mathbf{P}_a^2] \quad (1)$$

Table 4. Rotational parameters for the axial conformer of the pentamethylene sulfide \cdots HF complex.

	$\text{C}_5\text{H}_{10}\text{S} \cdots \text{HF}$	$\text{C}_5\text{H}_{10}^{34}\text{S} \cdots \text{HF}$	$^{13}\text{C}_\alpha\text{C}_4\text{H}_{10}\text{S} \cdots \text{HF}$	$^{13}\text{C}_\beta\text{C}_4\text{H}_{10}\text{S} \cdots \text{HF}$	$^{13}\text{C}_\gamma\text{C}_4\text{H}_{10}\text{S} \cdots \text{HF}$	$\text{C}_5\text{H}_{10}\text{S} \cdots \text{DF}$
A [MHz]	2078.08994(96) ^[a]	2052.739(15)	2058.102(16)	2059.618(16)	2068.823(15)	2076.199(14)
B [MHz]	1562.52189(70)	1559.7916(10)	1552.4213(10)	1550.97406(99)	1548.3744(12)	1544.59153(89)
C [MHz]	1471.28940(62)	1456.09099(89)	1467.76978(94)	1465.00301(88)	1454.07853(92)	1454.46690(87)
Δ_J [kHz]	1.6728(81)	1.6489(98)	1.6490(6)	1.6591(69)	1.6449(78)	1.6378(53)
Δ_{JK} [kHz]	−1.302(43)	−1.475(54)	−1.28(12)	−1.29(12)	−1.51(13)	−1.268(21)
Δ_K [kHz]	0.941(59)	[0.941] ^[b]	[0.941]	[0.941]	[0.941]	[0.941]
δ_J [kHz]	0.3572(47)	0.3686(72)	0.3452(75)	−0.3450(73)	−0.3486(78)	0.3461(71)
δ_K [kHz]	−5.15(16)	−4.52(19)	[−5.15]	[−5.15]	[−5.15]	[−5.15]
P_c ^[c] [u Å ²]	111.56895(61)	111.5612(16)	113.3905(16)	113.1267(16)	111.5585(16)	111.5707(15)
σ ^[d] [kHz]	3.1	2.2	1.7	2.1	1.1	1.8

[a] Standard error in parentheses in units of the last digit. [b] Parameters in square brackets were kept fixed in the fit. [c] $P_c = (I_a + I_b - I_c)/2 = \Sigma m_i r_i^2$. Conversion factor: $I_c \times C = 505379.1$ MHz u Å². [d] Root mean square (rms) deviation of the fit.

and $\Delta_J, \Delta_{JK}, \Delta_K, \delta_J$, and δ_K are the quartic centrifugal distortion constants. The rms deviation in the fits is below the estimated accuracy of the frequency measurements.

Equatorial PMS \cdots HF: It was clear from the early scans that the spectrum was denser than expected for a single conformer. Once all the transitions assigned to the axial conformer were discarded, the remaining transitions were assigned to the equatorial conformer. The $J = 5 \leftarrow 4$ set of transitions with the characteristic patterns arising from the K_{-1} substructure of a nearly prolate top was first identified in the frequency range 11.2–12.0 GHz. An initial fit of these transitions allowed the measurement of the remaining a -type R-branch lines of the parent species. No c -type transitions were observed, even though they were predicted. The spectrum of the equatorial conformer was found to be less intense than that of the axial form (eq:ax \approx 1:3). It should be noted that the intensity ratio remained unaltered when the carrier gas was changed from He to a heavier inert gas like Ar.

Hyperfine splittings generated by nuclear spin–nuclear spin interaction of the proton and fluorine nuclei within HF subunit could be resolved for some of the rotational transitions. The determination of the spectroscopic constants was then performed with a Hamiltonian of the form of Equation (2), where $H_R^{(A)}$ is defined in Equation (1) and $H_{SS} = \mathbf{I}_H \mathbf{D} \mathbf{I}_F$ is the Hamiltonian for the nuclear spin–nuclear spin interaction,^[21] where \mathbf{D} is the spin–spin coupling tensor. The Hamiltonian was evaluated in the coupled basis $\mathbf{I}_F + \mathbf{I}_H = \mathbf{I}, \mathbf{I} + \mathbf{J} = \mathbf{F}$. A direct diagonalisation procedure^[22] was used for

$$H = H_R^{(A)} + H_{SS} \quad (2)$$

the fitting of the measured transitions. The derived spectroscopic constants for the equatorial conformer are given in Table 6. Only the D_{aa} component of \mathbf{D} could be determined for the parent species. In all cases, the rms deviation of the fits lies in the range of the estimated accuracy of the frequency measurements. The measured transitions for the parent species are collected in Table 7. When hyperfine components were unresolved, the observed frequencies were assigned the quantum labels of the strongest predicted components.

Despite the weaker intensity of the spectra for the equatorial conformer, the high sensitivity of our spectrometer permitted the analysis of the ^{34}S and the three ^{13}C species in their natural abundance. The very low intensity spectra turn out to

Table 5. Rotational transitions [MHz] for the axial conformer of the pentamethylene sulfide...HF complex.

J'	K'_{-1}	K'_{+1}	J''	K''_{-1}	K''_{+1}	$\text{C}_5\text{H}_{10}\text{S}\cdots\text{HF}$		$\text{C}_5\text{H}_{10}^{34}\text{S}\cdots\text{HF}$		$^{13}\text{C}_\alpha\text{C}_4\text{H}_{10}\text{S}\cdots\text{HF}$		$^{13}\text{C}_\beta\text{C}_4\text{H}_{10}\text{S}\cdots\text{HF}$		$^{13}\text{C}_\gamma\text{C}_4\text{H}_{10}\text{S}\cdots\text{HF}$		$\text{C}_5\text{H}_{10}\text{S}\cdots\text{DF}$	
						obs	obs – calcd ^[a]	obs	obs – calcd	obs	obs – calcd	obs	obs – calcd	obs	obs – calcd	obs	obs – calcd
2	0	2	1	0	1	6056.493	0.001	6017.002	0.002							5987.541	–0.000
2	1	2	1	1	1	5976.333	–0.000	5928.012	0.000					5945.925	–0.000	5907.936	0.000
2	1	1	1	1	0	6158.817	0.001	6135.427	0.002	6124.998	0.003	6117.888	0.001			6088.203	–0.000
2	1	2	1	0	1	6491.894	0.001										
2	0	2	1	1	1	5540.932	0.001										
2	2	0	1	1	1	7807.836	–0.002										
2	2	1	1	1	0	7705.510	–0.001										
3	0	3	2	0	2	9057.999	0.001	8990.500	0.005	9022.156	0.001	9008.588	0.001			8955.835	0.001
3	1	3	2	1	2	8957.864	–0.000	8883.309	0.001	8927.636	0.002	8912.872	0.000	8858.838	–0.001	8855.583	–0.002
3	1	2	2	1	1	9230.697	–0.001	9193.063	–0.001	9180.864	–0.001	9170.036	–0.001	9140.796	–0.000	9125.172	0.001
3	2	2	2	2	1	9101.286	0.001	9047.507	0.002	9060.427	0.001					8997.032	0.003
3	2	1	2	2	0	9144.545	0.005	9104.477	–0.003	9098.666	–0.000	9086.954	0.006			9038.194	0.000
3	1	3	2	0	2	9393.268	0.002										
3	0	3	2	1	2	8622.597	0.001										
3	2	1	2	1	2	10976.048	0.003										
3	2	2	2	1	1	10647.980	–0.001										
4	0	4	3	0	3	12032.701	–0.007	11930.980	–0.004	11989.624	–0.004	11970.655	0.003	11901.914	0.002	11898.267	0.001
4	1	4	3	1	3	11932.559	–0.002	11829.884	–0.001	11893.494	0.002	11873.577	–0.001	11799.945	–0.001	11796.683	–0.001
4	1	3	3	1	2	12292.351	–0.000	12236.756	0.001	12227.776	–0.000	12212.998	–0.001	12171.598	0.001	12152.485	–0.000
4	2	3	3	2	2	12126.185	0.001	12051.629	0.001	12072.732	–0.000	12055.688	0.001	12000.281	0.001	11987.620	0.004
4	2	2	3	2	1	12228.233	–0.006			12163.402	–0.002	12148.469	–0.004	12107.699	0.001	12085.117	–0.001
4	3	2	3	3	1	12154.755	–0.008	12089.108	0.001							12014.840	–0.003
4	3	1	3	3	0	12159.802	0.001	12096.920	–0.003							12019.449	0.002
4	1	4	3	0	3	12267.831	0.003										
4	0	4	3	1	3	11697.438	–0.003										
4	3	1	3	2	2	14973.144	–0.001										
4	4	0	3	3	1	16065.393	0.003										
4	4	1	3	3	0	16064.485	–0.003										
5	0	5	4	0	4	14983.523	–0.004	14845.558	–0.002	14934.826	–0.003	14910.105	–0.004	14817.666	–0.001	14817.005	–0.003
5	1	5	4	1	4	14899.808	–0.001	14767.319	0.000	14852.624	0.000	14827.421	–0.000	14733.272	0.001	14730.586	0.001
5	1	4	4	1	3	15338.463	0.003	15258.991	–0.001	15261.135	0.002	15242.045	–0.001	15185.902	–0.002	15165.172	–0.001
5	2	4	4	2	3	15143.625	0.003	15045.946	–0.002	15078.431	–0.000	15056.824	–0.000	14985.478	0.000	14971.106	0.003
5	2	3	4	2	2	15327.889	0.003	15278.195	–0.002	15243.391	–0.001	15225.415	–0.000	15178.779	–0.002	15148.188	–0.004
5	3	3	4	3	2	15198.291	–0.000	15116.919	0.003							15023.312	0.001
5	3	2	4	3	1	15215.545	–0.001									15039.104	0.000
5	4	2	4	4	1	15193.078	–0.001									15018.096	–0.001
5	4	1	4	4	0	15193.505	–0.002									15018.472	–0.001
5	1	5	4	0	4	15134.932	0.003										
5	0	5	4	1	4	14748.412	0.004										
6	0	6	5	0	5	17920.407	–0.007	17748.365	0.001	17866.167	0.003	17835.644	0.002	17719.493	–0.000	17721.214	–0.000
6	1	6	5	1	5	17859.969	–0.002	17696.499	0.001	17805.257	–0.002	17774.650	0.001	17659.242	0.000	17657.556	–0.001
6	1	5	5	1	4	18362.663	–0.002	18251.223	–0.001	18275.387	–0.001	18251.483	0.001	18176.979	0.000	18157.242	–0.001
6	2	5	5	2	4	18152.042	–0.000	18028.559	–0.002	18076.120	0.001	18049.762	–0.001	17961.187	–0.001	17945.988	0.002
6	2	4	5	2	3	18431.145	–0.002	18370.626	0.004	18328.160	0.001	18306.970	0.002	18252.896	0.002	18216.037	0.001
6	3	4	5	3	3	18241.557	0.001	18143.340	0.003							18031.719	0.002
6	3	3	5	3	2	18285.739	0.004	18210.218	–0.003							18072.284	0.001
6	4	3	5	4	2	18238.730	–0.001									18028.428	0.000
6	4	2	5	4	1	18240.634	0.001									18030.099	–0.001
6	1	6	5	0	5	18011.380	0.006										
6	0	6	5	1	5	17769.015	0.002										

[a] Obs – calcd: observed – calculated values from the rotational parameters in Table 4.

Table 6. Rotational parameters for the equatorial conformer of the pentamethylene sulfide...HF complex.

	C ₅ H ₁₀ S...HF	C ₅ H ₁₀ ³⁴ S...HF	¹³ C _α C ₄ H ₁₀ S...HF	¹³ C _β C ₄ H ₁₀ S...HF	¹³ C _γ C ₄ H ₁₀ S...HF	C ₅ H ₁₀ S...DF
<i>A</i> [MHz]	2979.753(23) ^[a]	2948.822(29)	2947.335(26)	2951.572(25)	2968.433(27)	2981.005(25)
<i>B</i> [MHz]	1233.71575(71)	1226.40587(90)	1233.74033(85)	1225.59653(80)	1218.58997(81)	1215.18225(75)
<i>C</i> [MHz]	1092.44199(66)	1090.94656(78)	1088.06059(62)	1082.36200(62)	1082.11023(63)	1077.71185(62)
Δ_J [kHz]	1.4981(29)	1.4688(42)	1.4867(38)	1.4656(37)	1.4715(37)	1.4665(33)
Δ_{JK} [kHz]	−5.283(11)	−5.237(94)	−5.087(11)	−4.908(90)	−5.260(90)	−5.273(32)
Δ_K [kHz]	[0.0] ^[b]	[0.0]	[0.0]	[0.0]	[0.0]	[0.0]
δ_J [kHz]	−0.0884(36)	−0.0985(51)	−0.0828(38)	−0.0793(37)	−0.0888(37)	−0.0824(36)
δ_K [kHz]	[0.0]	[0.0]	[0.0]	[0.0]	[0.0]	[0.0]
<i>D</i> _{aa} [kHz]	−169(26)	—	—	—	—	—
<i>P</i> _b ^[c] [u Å] ²	111.2893(14)	111.2751(17)	113.1576(16)	112.8963(15)	111.2789(16)	111.2914(15)
σ ^[d] [kHz]	2.7	2.6	2.1	2.6	3.7	2.9

[a] Standard error in parentheses in units of the last digit. [b] Parameters in the square brackets were kept fixed in the fit. [c] $P_b = (I_a - I_b + I_c)/2 = \sum m_i b_i^2$. Conversion factor: $I_b \times B = 505379.1 \text{ MHz u Å}^2$. [d] Root mean square (rms) deviation of the fit.

be insufficient to resolve the nuclear spin–nuclear spin hyperfine structure, so only the central frequencies were considered in the fit. The rotational and quartic centrifugal distortion constants were then determined with the Hamiltonian of Equation (1) for all isotopic species and are given in Table 6. A selection of the central frequencies appears in Table 7.

Symmetry and structure: The symmetry of the axial and equatorial conformers was first established from simple considerations based on the values of the planar moments. The values of the planar moments P_c (axial) and P_b (equatorial) collected in Table 4 and Table 6, are almost equal and unchanged by isotopic substitution at ³²S(³⁴S), ¹²C(¹³C_γ) and H(D) atoms. Moreover, these values are nearly equal to P_b of free PMS, given in Table 2, which indicates that the *ab* and *ac* inertial planes of the axial and equatorial conformers, respectively, coincide with the *ac* symmetry plane of PMS. The small differences between the planar moments may be attributed to changes in zero-point motion on formation of the complexes. All of the above constitute conclusive experimental evidence for C_s symmetry in the axial and equatorial conformers.

Once the conformation was established, the *r*_o-like structures of the conformers were determined from a least-squares fit^[19] of the observed rotational constants. These were found to have a small dependence on the position of the H atom of HF. Consequently, a linear S...H–F hydrogen bond was first considered. The eighteen rotational constants from each conformer (given in Tables 4 and 6) yielded preliminary values of the structural parameters for both conformers. In the next step, the orientation of the HF subunit (and thus the position of the H atom), given by the angle α_{az} between the *a* principal inertial axis and the HF (*z*) bond (Figure 3) was estimated from the *D*_{aa} component of the spin–spin coupling tensor **D**. This value is related to the spin–spin coupling constant $D_0 = -286.75 \text{ kHz}$ of free HF^[23, 24] through Equation (3),^[25] where β is the oscillation angle of the HF subunit

$$D_a = (1/4) D_0 (3 \cos^2 \beta - 1) (3 \cos^2 \alpha_{az} - 1) \quad (3)$$

with respect to its centre of mass. For a wide range of hydrogen-bond complexes involving HF, this angle has been found to vary between 15° and 25°.^[25, 26] Taking an average

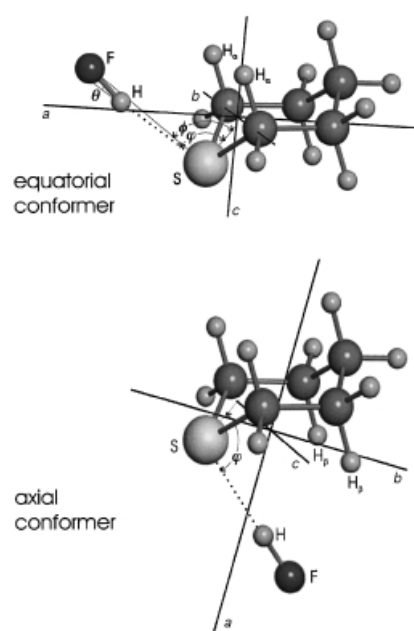


Figure 3. Structure of the equatorial and axial conformers of pentamethylene sulfide...HF, drawn to scale.

value of $\beta = 20(5)^\circ$, and considering the quoted error for *D*_{aa} (see Table 6), we estimated an α_{az} angle of $26(10)^\circ$ from Equation (3) for the equatorial conformer. For the axial conformer, a value of $D_{aa} = -28 \text{ kHz}$ has been estimated from Equation (3) considering the $\alpha_{az} = 51^\circ$ value obtained for the linear S...H–F hydrogen bond. The very small magnitude of the H–F nuclear spin hyperfine splittings predicted with this value of *D*_{aa} is consistent with the observation of nonresolvable experimental splittings for the axial conformer. Therefore, we can consider a nearly linear hydrogen bond configuration for this conformer.

Finally, fits were performed constraining the α_{az} angle to the above values of 26° and 51° for the equatorial and axial forms, respectively. The derived *r*_o-like structures for the axial and equatorial hydrogen-bond complexes are shown in Table 8 (see Figure 3 for definitions). The hydrogen-bond structure is described by the *r*(S...H) distance, the angle φ between the S...H line and the line bisecting the CSC angle and the angle θ that gives the deviation of the S...H–F system from a collinear arrangement. The derived value $\theta = 11(10)^\circ$ for the

Table 7. Rotational transitions [MHz] of the equatorial conformer of pentamethylene sulfide...HF complex.

J'	K'_{-1}	K'_{+1}	J''	K''_{-1}	K''_{+1}	I'	F'	I''	F''	$\text{C}_5\text{H}_{10}\text{S}\cdots\text{HF}^{[a]}$		$\text{C}_5\text{H}_{10}^{34}\text{S}\cdots\text{HF}^{[b]}$		$^{13}\text{C}_\alpha\text{C}_4\text{H}_8\text{S}\cdots\text{HF}^{[b]}$		$^{13}\text{C}_\beta\text{C}_4\text{H}_8\text{S}\cdots\text{HF}^{[b]}$		$^{13}\text{C}_\gamma\text{C}_4\text{H}_8\text{S}\cdots\text{HF}^{[b]}$		$\text{C}_3\text{H}_8\text{S}\cdots\text{DF}^{[b]}$	
										obs	obs – calcd ^[c]	obs	obs – calcd	obs	obs – calcd	obs	obs – calcd	obs	obs – calcd	obs	obs – calcd
3	0	3	2	0	2	1	4	1	3	6945.574	–0.001	6921.342	–0.001	6929.865	–0.000	6889.717	–0.002	6871.396	–0.003	6847.812	–0.000
3	1	3	2	1	2	1	4	1	3	6761.422	–0.002	6744.059	–0.000	6741.341	–0.002	6703.694	0.000	6692.571	–0.004	6667.646	0.001
3	1	2	2	1	1	1	4	1	3	7184.962	–0.001	7150.186	–0.001	7178.061	0.002	7133.095	–0.000	7101.761	–0.001	7079.801	–0.003
4	0	4	3	0	3	1	5	1	4	9223.574	0.001	9193.679	–0.000	9199.767	0.002	9147.735	–0.001	9127.083	–0.001	9095.445	0.001
4	1	4	3	1	3	1	5	1	4	9006.123	–0.001	8983.556	–0.001	8978.663	0.000	8928.828	0.001	8914.912	0.002	8881.627	–0.000
4	1	3	3	1	2	1	5	1	4	9569.464	–0.001	9523.810	–0.003	9559.385	–0.001	9499.893	–0.000	9459.253	–0.003	9429.924	–0.002
4	2	3	3	2	2	1	5	1	4	9298.012	0.002	9263.230	0.006	9280.056	–0.002	9224.959	–0.001	9196.623	0.005	9165.362	0.000
4	2	2	3	2	1	1	5	1	4	9378.681	0.000			9367.107	0.001	9308.678	0.004	9271.959	0.009	9241.114	0.003
4	3	2	3	3	1	1	5	1	4	9320.235	0.004										
4	3	1	3	3	0	1	5	1	4	9322.032	0.003										
5	0	5	4	0	4	1	6	1	5	11473.245	0.001	11439.366	0.002	11439.507	0.005	11376.556	0.003	11356.072	0.002	11316.222	0.002
5	1	5	4	1	4	1	6	1	5	11243.869	–0.001	11216.521	–0.002	11208.546	–0.001	11146.780	–0.002	11130.708	–0.001	11089.034	–0.001
5	1	4	4	1	3	1	6	1	5	11944.062	–0.001	11888.227	–0.002	11929.930	–0.001	11856.366	–0.002	11807.551	–0.004	11770.805	–0.002
5	2	4	4	2	3	1	6	1	5	11611.963	–0.004	11715.778	0.003	11588.692	–0.003	11520.262	0.001	11485.922	–0.000	11446.796	–0.005
5	2	3	4	2	2	1	6	1	5	11768.695	0.002	11569.175	–0.000	11757.369	0.001	11682.691	0.002	11632.551	–0.003	11594.258	0.003
						1	5	1	4	11768.683	–0.002										
5	3	3	4	3	2	1	6	1	5	11655.790	0.001									11488.006	0.002
						1	5	1	4	11655.770	–0.001										
5	3	2	4	3	1	1	6	1	5	11662.052	0.001									11493.668	0.003
						1	5	1	4	11662.035	0.000										
6	0	6	5	0	5	1	7	1	6	13694.024	0.003	13657.588	0.003	13649.049	–0.001	13575.868	–0.003	13557.470	0.003	13509.233	0.006
6	1	6	5	1	5	1	7	1	6	13473.905	0.000	13442.218	–0.001	13430.241	–0.001	13356.798	–0.003	13339.223	–0.001	13289.117	–0.002
6	1	5	5	1	4	1	7	1	6	14305.137	–0.001	14240.098	0.002	14285.711	–0.002	14198.729	–0.001	14143.328	–0.002	14099.102	0.000
6	2	5	5	2	4	1	7	1	6	13918.948	–0.007	13868.610	–0.003	13889.824	0.002	13808.340	0.000	13768.709	–0.005	13721.688	–0.006
6	2	4	5	2	3	1	7	1	6	14180.263	0.001	14113.586	0.000			14078.597	–0.001	14013.899	0.006	13968.284	0.003
						1	6	1	5	14180.255	–0.003										
6	3	4	5	3	3	1	7	1	6	13993.530	0.001									13791.903	–0.001
6	3	3	5	3	2	1	7	1	6	14010.093	0.005									13806.887	0.004
6	4	3	5	4	2	1	7	1	6	13984.559	0.002										
						1	6	1	5	13984.543	0.003										
6	4	2	5	4	1	1	7	1	6	13984.882	–0.001										
						1	6	1	5	13984.867	0.001										
7	0	7	6	0	6	1	8	1	7	15890.301	0.004	15852.128	0.003	15833.783	0.001	15750.570	0.005	15734.965	0.004	15678.153	0.001
7	1	7	6	1	6	1	8	1	7	15695.990	–0.003	15660.387	–0.001	15643.569	0.000	15558.684	0.005	15540.185	–0.003	15481.605	–0.002
7	1	6	6	1	5	1	8	1	7	16648.408	–0.001	16575.457	–0.002	16622.015	–0.003	16522.487	–0.000	16462.644	–0.000	16410.855	–0.001
7	2	6	6	2	5	1	8	1	7	16217.690	–0.007	16160.332	–0.004	16597.577	0.003	16087.872	–0.004	16043.786	–0.006	15988.826	–0.006
7	2	5	6	2	4	1	8	1	7	16607.371	0.004	16526.710	0.003			16489.834	0.003	16410.776	0.003	16357.989	0.003
7	3	5	6	3	4	1	8	1	7	16332.589	–0.004									16097.162	–0.003
7	3	4	6	3	3	1	8	1	7	16369.326	0.004									16130.425	0.001
7	4	4	6	4	3	1	8	1	7	16322.803	0.003										
7	4	3	6	4	2	1	8	1	7	16323.883	0.002										
7	5	3	6	5	2	1	8	1	7	16312.157	–0.004										
7	5	2	6	5	1	1	8	1	7	16312.171	–0.004										
8	0	8	7	0	7									18002.418	0.002	17908.893	0.003	17895.624	0.004	17830.093	0.004
8	1	8	7	1	7	1	9	1	8	17910.377	0.001			17848.866	–0.003	17752.704	–0.005	17733.778	–0.003	17666.677	–0.002

[a] Unresolved components were assigned the quantum label of the strongest predicted component. [b] Applicable labelling only by J' , K'_{-1} , K'_{+1} , J'' , K''_{-1} and K''_{+1} quantum numbers. [c] Obs – calcd: Observed – calculated values from the rotational parameters in Table 6.

Table 8. Experimental structural parameters for axial and equatorial conformers in pentamethylene sulfide...HF complexes.

Parameters ^[a,b]	PMS...HF axial	PMS...HF equatorial
$r(\text{X}\cdots\text{S})$ [Å]	3.114(4) ^[c]	3.10(2)
$r(\text{H}\cdots\text{S})$ [Å]	2.19(1)	2.18(2)
ϕ [°]	101.8(5)	91.(2)
φ [°]	101.8(5)	95.(4)
θ [°]	[0.0] ^[d]	11.(10)
$r(\text{X}\cdots\text{H}_a)$ [Å]		3.15(3)
$r(\text{X}\cdots\text{H}_\beta)$ [Å]	2.81(2)	
$r(\text{S}\cdots\text{C}_a)$ [Å]	1.812(8)	1.81(3)
$r(\text{C}_a\cdots\text{C}_\beta)$ [Å]	1.524(9)	1.52(2)
$r(\text{C}_\beta\cdots\text{C}_\gamma)$ [Å]	1.52(1)	1.54(1)
$\angle \text{C}_a\text{SC}_\alpha$ [°]	98.6(5)	97.(2)
$\angle \text{SC}_\alpha\text{C}_\beta$ [°]	112.9(6)	112.(2)
$\angle \text{C}_\alpha\text{C}_\beta\text{C}_\gamma$ [°]	112.1(9)	112.(1)
$\angle \text{C}_\beta\text{C}_\gamma\text{C}_{\beta'}$ [°]	112.3(8)	113.(1)
ξ [°]	132.0(7)	129.(3)
ζ [°]	126.(1)	127.(2)

[a] See Figures 2 and 3 for notation. [b] The remaining parameters were kept fixed at standard values of $r(\text{C}\cdots\text{H}) = 1.095$ Å and $\angle \text{HCH} = 108.5^\circ$ (with a C_{2v} local symmetry around the C atoms). [c] Standard errors in parentheses in units of the last digit. [d] Parameter kept fixed.

equatorial conformer is also consistent with a linear arrangement for the $\text{S}\cdots\text{H}\cdots\text{F}$ system.

With the aim of complementing the experimental data, we performed ab initio calculations on the two axial and equatorial conformers. All quantum-mechanical calculations were made with the Gaussian 98 suite of programs^[27] at the MP2/6-311 + G(d,p) level of theory, which has been found to behave satisfactorily for related complexes.^[5, 10, 28, 29] Full geometry optimisations were executed with C_s symmetry as the only constraint. The calculated near-equilibrium structures for both conformers are collected in Table 9. The theoretical values agree satisfactorily with the experimental

Table 9. Experimental and MP2/6-311 + G(d,p) optimised parameters for the equatorial and axial pentamethylene sulfide...hydrogen fluoride complex.

	$\text{C}_5\text{H}_{10}\text{S}\cdots\text{HF}$ equatorial		$\text{C}_5\text{H}_{10}\text{S}\cdots\text{HF}$ axial	
	Experimental	Ab initio	Experimental	Ab initio
A [MHz]	2979.753(23) ^[a]	3058.	2078.08994(96)	2075.
B [MHz]	1233.71575(61)	1206.	1562.52189(70)	1564.
C [MHz]	1092.44199(66)	1063.	1471.28940(62)	1466.
$P_{\text{b,c}}$ ^[b] [u Å] ²	111.2893(14)	111.	111.56895(61)	111.
ΔE [kJ mol ⁻¹]		-32.4		-34.4
$\Delta E(\text{CP})$ [kJ mol ⁻¹]		-27.1		-27.9
$\Delta E(\text{BSSE})$ [kJ mol ⁻¹]		-26.0		-26.4
μ_a [D] ^[c]		3.95		3.52
μ_b [D]		0.0		0.93
μ_c [D]		0.08		0.0
μ_T [D]		3.95		3.64
$r(\text{X}\cdots\text{S})$ [Å]	3.10(2)	3.10	3.114(4)	3.11
$r(\text{H}\cdots\text{S})$ [Å]	2.18(2)	2.18	2.19(1)	2.18
ϕ [°]	91.(2)	94.	101.8(5)	102.
φ [°]	95.(4)	98.	101.8(5)	104.
θ [°]	11.(10)	12.	0.	6.
$r(\text{X}\cdots\text{H}_a)$ [Å]	3.15(3)	3.23		
$r(\text{X}\cdots\text{H}_\beta)$ [Å]			2.81(2)	2.83

[a] Standard errors in parentheses are given in units of the last digits. [b] $P_b = (I_a - I_b + I_c)/2 = \Sigma m_i b_i^2$ value for the equatorial form and $P_c = (I_a + I_b - I_c)/2 = \Sigma m_i c_i^2$ value for the axial form. Conversion factor: $I_b \times B = 505379.1 \text{ MHz u Å}^2$. [c] $1 \text{ D} \cong 3.33564 \times 10^{-30} \text{ C m}$.

structure. The very small value predicted for the μ_c dipole moment component in the equatorial conformer is also consistent with the fact that no c -type spectrum was observed. The stabilisation energies and corrected values are also shown in Table 8. ΔE corresponds to the uncorrected values for the stabilisation energies. Possible basis set superposition error (BSSE)^[30] was estimated by the counterpoise (CP) procedure,^[31] including fragment relaxation energy terms.^[32] The ab initio energy difference between the two conformers is very small. The axial form appears to be the most stable, in agreement with the experimental results.

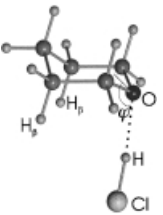

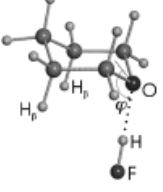
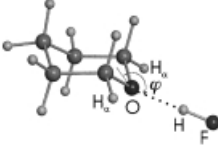
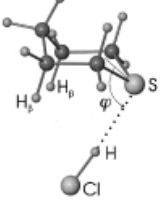
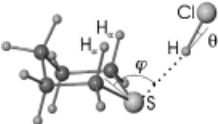
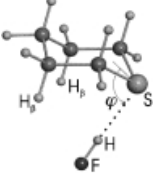

Discussion

The observation in a supersonic jet of both axial and equatorial conformers is conclusive experimental evidence that the two nonbonding electron pairs at the sulfur atom are nonequivalent as a result of the chair conformation of the ring. Analysis of the spectroscopic constants from all observed isotopic species allowed us to determine the effective structures for both conformers. The structural parameters in Table 8 corresponding to the PMS subunit in both axial and equatorial forms can be compared with those of the bare monomer that appear in Table 3. The very close similarity between them is a strong indication that the geometry of the thioether PMS is not altered upon complexation. The same conclusion has also been reached in studies of THP...HF,^[5] oxetane...HF^[9] and 7-oxabicyclo[2.2.1]heptane...HF.^[33] The structure of the monomer survives complex formation as usually assumed.

The hydrogen bond lengths $r(\text{S}\cdots\text{H})$ and φ angles (see Figure 3) derived for the axial and equatorial conformers are very close to those obtained in the related five-membered-ring tetrahydrothiophene...HF complex.^[13] The $r(\text{S}\cdots\text{H})$ distances around 2.2 Å and φ values in the range 90–100° suggest a configuration with a *near*-local C_{2v} symmetry around the S atom in these cyclothioethers. On this basis, the structures of both conformers can be rationalised in terms of a simple electrostatic model involving the interaction of the axial and equatorial lone electron pairs on S with the electrophilic region $\delta^+\text{H}$ of the HF molecule. Consequently, the direction of HF in the complex can be taken as a probe for the orientation of these nonbonding electron pairs^[34] of the S atom. The axis of these pairs in PMS appears to be nearly perpendicular to the CSC plane. This configuration would also be expected in terms of an interaction between the σ^* LUMO orbital of HF and n_π HOMO orbital of PMS, which is perpendicular to the CSC plane owing to its 3p character.

The hydrogen bond parameters are compared in Table 10 with those reported for the axial and equatorial hydrogen bond complexes formed between THP and PMS with HX ($\text{X} = \text{Cl}, \text{F}$). The hydrogen bond lengths $r(\text{S}\cdots\text{H})$ and $r(\text{O}\cdots\text{H})$ are longer for the axial conformers in all the complexes. If we accept that the strength of the hydrogen bond is related to the hydrogen bond length, it can be concluded that the equatorial is the strongest primary hydrogen bond in all cases. In contrast, with the exception of the PMS...HCl complex, a

Table 10. Hydrogen bond properties for tetrahydropyran and pentamethylene sulfide \cdots HX complexes.

	$r(\text{S/O} \cdots \text{H})$ [Å]	φ [°]	$r(\text{X} \cdots \text{H}_{\alpha/\beta})$ [Å]	Carrier gas	Ratio	Relaxation of conformer	$\nless n\text{Bn}^{[a]}$ [°]
	1.85(2) ^[b]	126.(1)	3.41(3)	Ar, He	$\frac{10}{1}$	↑ Yes	95.7
	1.74(2)	138.(1)	3.83(3)	He			
	1.67(2)	130.7(8)	3.11(3)	Ar, He	$\frac{40}{1}$	↑ Yes	81.2
	1.62(4)	148.(1)	3.40(3)	He			
	2.35(8)	100.(2)	3.12	Ar, He	$\frac{1}{4}$	⚡ No	161.9
	2.19(5)	98.(1)	3.34	Ar, He			
	2.19(1)	101.8(5)	2.81(2)	Ar, He	$\frac{3}{1}$	⚡ No	171.1
	2.18(2)	95.(4)	3.15(3)	Ar, He			

[a] $\nless n\text{Bn} = 360^\circ - (\varphi_{\text{ax}} + \varphi_{\text{eq}})$. [b] Standard errors in parentheses in units of the last digit.

preference for the axial conformer has been found experimentally. Secondary interactions have to be invoked to explain these experimental results.

Secondary hydrogen-bond interactions between the $\delta\text{-X}$ of HX and the nearest H_α or H_β atoms of the methylenic groups of the ring become apparent when distortions in the natural linearity of the primary hydrogen bond are observed. In this way, the significant nonlinearity observed in the equatorial

conformer of $\text{PMS} \cdots \text{HCl}$ complex (see Table 10) has been interpreted in terms of those interactions. An important characteristic of secondary interactions is the distance between the interacting atoms; for HF complexes these fall in the range 2.8–3.2 Å as reported for related complexes,^[5, 9, 11, 13, 25, 26, 33, 35] while for complexes with HCl,^[3, 4, 6, 8, 10, 12, 36, 37] typical distances are 3.1–3.6 Å. For $\text{PMS} \cdots \text{HCl}$, the distances between the $\delta\text{-F}$ of HF and the

nearest H_α or H_β atoms of the PMS ring (Figure 3) have been calculated to be 3.15 Å and 2.81 Å, for the equatorial and axial conformers, respectively. Thus, in this case, the linear hydrogen bonds are compatible with the existence of secondary interactions.

The intensity ratio (ax:eq ≈ 3:1) obtained from the *a*-type rotational spectra of axial and equatorial conformers cannot be imputed to differences in the values of the electric dipole moments; ab initio calculations give similar values for the μ_a dipole moment components for both conformers (see Table 9). Thus, a slightly more stable axial form can be inferred from the observed intensities. The very similar values of the stabilisation energies from the ab initio calculations support this point. An interesting question to answer is how the secondary interactions control the axial–equatorial conformational preference. In the case of THP...HF and THP...HCl complexes the values of the $r(\text{F}\cdots\text{H}_{\alpha/\beta})$ distances reveal the existence of secondary hydrogen bonds only for the axial conformer, a fact clearly reflected in their intensity ratios ax:eq of about 10:1 and 40:1, respectively. In PMS...HF the $r(\text{F}\cdots\text{H}_{\alpha/\beta})$ distances in the axial and equatorial forms make possible the presence of second-order interactions in both conformers. In addition, the shorter value of 2.81 Å for the axial conformer (with respect to that of 3.15 Å calculated for the equatorial conformer) would favour the axial conformer, if we accept that a shortening in the bond length is related to an increase in bond strength. Thus, the relative stability (ax:eq ≈ 3:1) found in the PMS...HF complex can be understood in terms of a delicate balance between the effects of primary and secondary hydrogen bonds. Same arguments can be used to explain the intensity ratio (ax:eq ≈ 1:4) observed in the PMS...HCl complex.^[4]

Another interesting point to discuss is the dependence of the intensity ratio of the axial and equatorial conformers on the carrier gas used in the supersonic expansion. In THP complexes with HCl^[3] and HF^[5] the least stable equatorial conformer could only be detected when He was used as carrier gas, while the axial form was readily observed with both Ar and He. In contrast, this behaviour is not displayed by the related complexes PMS...HCl^[4] and PMS...HF, in which the intensity ratio between the axial and the equatorial conformers remains qualitatively the same regardless of which of the two carrier gases. To explain these striking experimental features it is postulated that the inert carrier gas produces relaxation from the high-energy form to the most stable one owing to collisions with the He or Ar atoms. It has been reported that this phenomenon is observed when the barrier height to interconversion between the conformers is lower than a certain value (about 400 cm⁻¹)^[38] and the relaxation takes place with greater efficiency when a heavier inert gas (like Ar) is used. The relaxation can proceed by two different interconversion paths: inversion of the HX molecule or of the six-membered ring itself. The conformer relaxation through ring inversion is expected to be hindered by a very high barrier,^[39] so the conformer interconversion would only take place through an inversion of HX between the two nonequivalent binding sites around the O or S atoms. The angle $\angle \text{nBn}$ (B = O, S) between the lone pairs could also be correlated with the barrier to inversion. In the PMS...HX

complexes, a relatively high barrier exists for conversion of the equatorial conformer into the axial one because of the large angle between the nonbonding electron pairs (close to 180°). Consequently, vibrational relaxation is incomplete in the adiabatic expansion of the experiment and the high-energy conformer is trapped within its individual well. Thus, both axial and equatorial conformers are observable in these low-temperature experiments, independently of the carrier gas used. Alternatively, the significantly smaller values of $\angle \text{nBn}$ angles in THP...HX complexes (close to 90°) can explain the observed experimental relaxation (see Table 10). Recently, a very low barrier (100 cm⁻¹) for the inversion of HF has been determined in the related five-membered ring 2,5-dihydrofuran...HF complex,^[40] with a $\angle \text{nBn}$ angle of 91°, which corroborates the above conclusions.

Experimental Section

A molecular beam Fourier transform microwave spectrometer^[14] (MB-FTMW) operating in the frequency range 5.5–18.5 GHz was used to record the rotational spectra. The pentamethylene sulfide (PMS)...HF complex was generated by adiabatic expansion of gas mixtures of PMS (0.5%) and HF or DF (1%) in He or Ar at total pressures of ≈ 2 bar. The ¹³C and ³⁴S isotopic species were observed in their natural abundances. DF was prepared by saturating the walls of a lecture bottle with D₂O, which was then filled with HF at a pressure of about 1 bar. All experimental conditions were optimised to obtain the best signal/noise ratio. The frequency domain spectrum was obtained after Fourier transformation of the 8 k data points in the time domain signal. Since the molecular beam is introduced parallel to the microwave radiation, each transition is split into two components because of the Doppler effect. The resonance frequency is taken as the mean value of the Doppler components. The estimated accuracy of the frequency measurements is better than 5 kHz.

Acknowledgement

The authors would like to thank the Ministerio de Ciencia y Tecnología (DGI Grant BQU2000-0869), the Junta de Castilla y León (Grants VA41/00B and VA017/01) and the Fundación Ramon Areces for funds.

- [1] J. M. Hollas in *Jet Spectroscopy and Molecular Dynamics* (Eds.: J. M. Hollas, D. Phillips), Chapman & Hall, Glasgow, **1995**.
- [2] T. J. Balle, W. H. Flygare, *Rev. Sci. Instrum.* **1981**, *52*, 33–45.
- [3] S. Antolínez, J. C. López, J. L. Alonso, *Angew. Chem.* **1999**, *111*, 1889–1892; *Angew. Chem. Int. Ed.* **1999**, *38*, 1772–1774.
- [4] M. E. Sanz, J. C. López, J. L. Alonso, *Chem. Eur. J.* **1999**, *5*, 3293–3298.
- [5] S. Antolínez, J. C. López, J. L. Alonso, *Chem. Phys. Chem.* **2001**, *2*, 114–117.
- [6] S. Antolínez, A. Lesarri, J. C. López, J. L. Alonso, *Chem. Eur. J.* **2000**, *6*, 3345–3350.
- [7] M. E. Sanz, A. Lesarri, J. C. López, J. L. Alonso, *Angew. Chem.* **2001**, *113*, 961–964; *Angew. Chem. Int. Ed.* **2001**, *40*, 935–938.
- [8] S. Antolínez, J. C. López, J. L. Alonso, *Chem. Phys. Lett.* **2001**, *334*, 250–256.
- [9] M. E. Sanz, V. M. Sanz, J. C. López, J. L. Alonso, *Chem. Phys. Lett.* **2001**, *342*, 31–38.
- [10] J. C. López, J. L. Alonso, F. J. Lorenzo, V. M. Rayón, J. A. Sordo, *J. Chem. Phys.* **1999**, *111*, 6363–6374.
- [11] J. L. Alonso, J. C. López, S. Blanco, A. Lesarri, F. J. Lorenzo, *J. Chem. Phys.* **2000**, *113*, 2760–2767.
- [12] M. E. Sanz, J. C. López, J. L. Alonso, *J. Phys. Chem. A* **1998**, *102*, 3681–3689.

- [13] M. E. Sanz, J. C. López, J. L. Alonso, *Chem. Phys. Lett.* **1998**, 288, 760–766.
- [14] J. L. Alonso, F. J. Lorenzo, J. C. López, A. Lesarri, S. Mata, H. Dreizler, *Chem. Phys.* **1997**, 218, 267–275.
- [15] R. W. Kitchin, T. B. Malloy Jr., R. L. Cook, *J. Mol. Spectrosc.* **1975**, 57, 179–188.
- [16] J. C. López, J. L. Alonso, R. M. Villamañán, *J. Mol. Struct.* **1986**, 147, 67–76.
- [17] J. K. G. Watson in *Vibrational Spectra and Structure*, Vol. 6 (Ed.: J. R. Durig), Elsevier, Amsterdam, **1977**, pp. 1–89.
- [18] J. Kraitichman, *Am. J. Phys.* **1953**, 21, 17–24.
- [19] H. D. Rudolph, *Struct. Chem.* **1991**, 2, 581–588.
- [20] G. Guelachvili, *Opt. Comm.* **1976**, 19, 150–154.
- [21] W. G. Read, W. H. Flygare, *J. Chem. Phys.* **1982**, 76, 2238–2246.
- [22] H. M. Pickett, *J. Mol. Spectrosc.* **1991**, 148, 371–377.
- [23] J. S. Muentner, W. Kemplerer, *J. Chem. Phys.* **1970**, 52, 6033–6037.
- [24] J. S. Muentner, *J. Chem. Phys.* **1972**, 56, 5409–5412.
- [25] A. C. Legon, A. L. Wallwork, D. J. Millen, *Chem. Phys. Lett.* **1991**, 178, 279–284.
- [26] M. J. Atkins, A. C. Legon, H. E. Warner, *Chem. Phys. Lett.* **1994**, 229, 267–272.
- [27] Gaussian 98, Revision A.7, Gaussian, Pittsburgh, PA (USA), **1998**.
- [28] H. Valdés, V. M. Rayón, J. A. Sordo, *Chem. Phys. Lett.* **2000**, 320, 507–512.
- [29] H. Valdés, J. A. Sordo, *Chem. Phys. Lett.* **2001**, 333, 169–180.
- [30] B. Liu, A. D. McLean, *J. Chem. Phys.* **1973**, 59, 4557–4558.
- [31] S. F. Boys, F. Benardi, *Mol. Phys.* **1970**, 19, 553–566.
- [32] S. S. Xanteas, *J. Chem. Phys.* **1996**, 104, 8821–8824.
- [33] S. Antolínez, M. Gerbi, J. C. López, J. L. Alonso, *Phys. Chem. Chem. Phys.* **2001**, 3, 796–799.
- [34] A. C. Legon, D. J. Millen, *Chem. Soc. Rev.* **1987**, 16, 467–498.
- [35] J. Cosléou, D. G. Lister, A. C. Legon, *Chem. Phys. Lett.* **1994**, 231, 151–158.
- [36] A. C. Legon, C. A. Rego, A. L. Wallwork, *Chem. Phys. Lett.* **1992**, 97, 3050–3059.
- [37] S. Antolínez, S. Blanco, J. C. López, J. L. Alonso, *Phys. Chem. Chem. Phys.* **2000**, 2, 4658–4662.
- [38] R. S. Ruoff, T. D. Klots, T. Emilsson, H. S. Gutowsky, *J. Chem. Phys.* **1990**, 93, 3142–3150.
- [39] H. M. Pickett, H. L. Strauss, *J. Am. Chem. Soc.* **1970**, 92, 7281–7290.
- [40] J. C. López, S. Blanco, A. Lesarri, M. E. Sanz, F. J. Lorenzo, J. L. Alonso, *J. Chem. Phys.* **2001**, 114, 9421–9429.

Received: September 20, 2001 [F3566]